

MEDGPT-OSS: TRAINING A GENERAL-PURPOSE VISION-LANGUAGE MODEL FOR BIOMEDICINE

Kai Zhang¹, Zhengqing Yuan², Cheng Peng³, Songlin Zhao¹, Mengxian Lyu³, Ziyi Chen³, Yanfang Ye², Wei Liu⁴, Ying Zhang⁵, Kaleb E Smith⁶, Lifang He¹, Lichao Sun^{1,*}, Yonghui Wu^{3,*}

¹Department of Computer Science and Engineering, Lehigh University

²Department of Computer Science and Engineering, University of Notre Dame

³Department of Health Outcomes & Biomedical Informatics, University of Florida

⁴Department of Radiation Oncology, Mayo Clinic

⁵Research Computing, University of Florida

⁶AI Technology Center, NVIDIA

lis221@lehigh.edu, yonghui.wu@ufl.edu

ABSTRACT

Biomedical multimodal assistants have the potential to unify radiology, pathology, and clinical-text reasoning, yet a critical deployment gap remains: top-performing systems are either closed-source or computationally prohibitive, precluding the on-premises deployment required for patient privacy and PHI compliance. We introduce MEDGPT-OSS, an open-weight, 20B-parameter generalist vision-language model designed to facilitate open research in clinical AI. Rather than relying on architectural complexity, MEDGPT-OSS pairs the GPT-oss language backbone with a visual front-end via a optimized, three-stage training curriculum. By progressively domain-adapting these modules through rigorous data curation and long-context multimodal alignment, we demonstrate that a 20B model can bridge the capacity gap. It successfully outperforms larger open medical models on out-of-distribution (OOD) multimodal reasoning and complex text-only clinical tasks. By unifying diverse modalities under a single instruction-following interface, MEDGPT-OSS maintains a parameter-efficient footprint fully compatible with commodity GPUs. We release the complete training recipe, open-weight checkpoints, and a rigorous evaluation harness to serve as a verifiable foundation for privacy-preserving, institution-specific clinical AI research.

1 INTRODUCTION

Biomedical AI has made rapid progress across image interpretation, clinical-text understanding, and multimodal reasoning Thirunavukarasu et al. (2023). Yet, most deployed systems remain specialists: models trained for a single task and often a single modality Moor et al. (2023). This specialization complicates real-world clinical use, where decision-making is inherently multimodal and longitudinal, requiring the continuous integration of radiographs, pathology slides, and patient narratives over time.

Recent “generalist” vision-language models (VLMs) aim to unify these heterogeneous inputs within a single backbone. However, the most capable systems are predominantly closed-source, precluding the on-premises deployment required to satisfy strict safety auditing and data privacy (PHI) mandates. While open-weight medical VLMs have emerged to address this Liu et al. (2023b); Zhang et al. (2024), the field faces a delicate trade-off between scaling for complex reasoning and maintaining practical deployability. Smaller models (e.g., 7B) often lack the capacity for rigorous multi-step clinical logic, whereas larger models present elevated serving costs and memory bottlenecks for standard IT infrastructure. Furthermore, many current approaches assume that bridging this gap requires initializing from computationally expensive, pre-existing domain-specific vision encoders.

*Corresponding authors.

In this technical report, we introduce MEDGPT-OSS, an open-weight, 20B-parameter generalist biomedical VLM designed to address the challenge of balancing advanced clinical reasoning with accessible deployment. Starting with the robust GPT-oss language backbone Agarwal et al. (2025) and a standard CLIP Radford et al. (2021) visual encoder connected via a simple linear projector, we establish that architectural minimalism—when supported by an optimized, progressive training curriculum—is remarkably effective. By continuously updating the visual and projection weights alongside the language model during our alignment and mid-training phases, we demonstrate that a systematic data recipe can dynamically adapt general-purpose modules to the medical domain, achieving frontier-level multimodal alignment without relying on bespoke architectural engineering.

MEDGPT-OSS-20B demonstrates highly competitive performance across multiple challenging benchmarks. Notably, it matches or exceeds the performance of larger open-sourced models in nearly half of our evaluations (8 of 17) focusing on complex, multi-step clinical reasoning and multimodal in-context learning. Furthermore, it exhibits a robust ability to resist negative transfer when provided with unseen clinical demonstrations. This parameter-efficient footprint ensures the model is fully compatible with commodity GPUs, enabling seamless on-premises fine-tuning and inference. In summary, our contributions are as follows:

- **A unified, multi-stage training recipe:** We detail a fully reproducible, three-stage curriculum (short-context alignment, long-context mid-training, and mixed instruction tuning) that progressively domain-adapts general-purpose vision and language modules. This pipeline proves that strategic data curation and joint parameter updating can empower a 20B model to punch significantly above its weight class, eliminating the strict dependency on specialized vision encoders.
- **SOTA empirical performance:** MEDGPT-OSS-20B establishes new state-of-the-art results among open models on challenging OOD benchmarks (e.g., MedFrameQA, MedXQA). Notably, it crosses the reasoning threshold required for complex clinical QA, outperforming 30B+ systems in both zero-shot and few-shot generalization.
- **Accessible clinical deployment:** By releasing our open-weight checkpoints, comprehensive data recipes, and standardized evaluation harnesses, we provide a complete ecosystem for on-premises, air-gapped clinical deployment. This enables healthcare institutions to conduct rigorous, privacy-preserving validation without exporting sensitive patient data.

This report positions MEDGPT-OSS not as a finalized clinical oracle, but as a highly capable, transparent foundation for the medical AI research community to build upon, audit, and deploy safely. Our ongoing work focuses on developing larger models and integrating advanced techniques to further the development of open, reliable medical AI.

2 RELATED WORK

Specialist pipelines and their limits. Early biomedical AI largely advanced through modality- and task-specific pipelines. In radiology, report generation commonly followed encoder-decoder designs that map images to long-form text, but generation quality is often sensitive to supervision biases and prone to omission or hallucination when summarizing complex findings (Johnson et al., 2019). Medical VQA developed with task-specific models that frequently reduce answering to classification over constrained spaces, limiting expressivity and robustness under distribution shift (Lau et al., 2018; Liu et al., 2021). In computational pathology, weakly supervised multiple-instance learning became a standard recipe for whole-slide understanding, but it is typically vision-only and tightly coupled to slide-level supervision, making cross-task transfer and multimodal grounding difficult (Lu et al., 2021). Clinical NLP similarly evolved as text-only models tailored to individual supervised objectives (e.g., clinical NLI), which often generalize poorly beyond their training distributions (Romanov & Shivade, 2018). Across these silos, recurring bottlenecks include limited cross-task transfer, weak multimodal integration, and unreliable long-form generation (Yang et al., 2022).

Generalist biomedical VLMs and instruction-tuned assistants. A key inflection point was the move from per-task systems toward generalist biomedical vision-language modeling.

Representation- and retrieval-oriented pretraining (e.g., large-scale biomedical image-text contrastive learning) improved transfer across diverse downstream tasks and enabled stronger cross-modal alignment (Zhang et al., 2025b). Generalist architectures that unify heterogeneous biomedical tasks under a single model further reduced task fragmentation and improved cross-task reuse (Zhang et al., 2024; Peng et al., 2025). In parallel, domain instruction tuning of general-purpose multimodal assistants demonstrated that a strong base model can be specialized into a medically useful interactive assistant with relatively lightweight post-training (Liu et al., 2023b). Beyond biomedical-first models, unified multimodal backbones (e.g., sequence-to-sequence formulations) provided effective starting points for medical adaptation. Together, these lines shifted emphasis from designing task-specific heads to building reusable multimodal interfaces and training recipes that support broader coverage and transfer.

Frontier trends: recipes, long-context grounding, and evaluation. Recent work pushes generalist medical MLLMs further by treating *training and evaluation recipes* as first-class: multi-stage curricula that combine continued pretraining with instruction tuning, higher-quality and more diverse medical mixtures (including synthetic instructions/reasoning traces), longer-context multimodal grounding, and stronger reliability-oriented evaluation toolkits and protocols (Jiang et al., 2025; Xu et al., 2025; Sellergren et al., 2025; Ossowski et al., 2025; Dai et al., 2025). Closed systems often report strong zero-/few-shot performance and long-context capabilities, but limited disclosure constrains reproducibility and independent auditing (Tu et al., 2023; OpenAI, 2023). Overall, the field is converging on a performance–transparency–deployability frontier, where progress increasingly depends on reproducible recipes and standardized, reliability-aware evaluation rather than benchmark scores alone.

Positioning of MEDGPT-OSS. MEDGPT-OSS targets a practical open-weight regime motivated by privacy and governance constraints in clinical deployment: open weights and permissive licensing support on-premises and even air-gapped use, enabling institution-specific adaptation without exporting PHI. To ensure reproducibility and reliable comparison, we disclose training recipes and evaluation code, prevent train–test overlap to avoid leakage, and standardize benchmarking via a unified inference harness with deterministic decoding and strict, fully automated scoring rules. Methodologically, we adopt a simple three-stage curriculum (short alignment → long-context mid-training → mixed multimodal/text instruction tuning). Finally, we emphasize reliability-oriented evaluation by combining standardized automatic scoring with task-specific, clinically informed assessment protocols, aligning model development with externally valid reporting.

3 MEDGPT-OSS

In the following, we delineate the design of MEDGPT-OSS across three fundamental pillars: (a) model architecture, (b) training strategies, and (c) implementation details (e.g., hyperparameter selection).

3.1 MODEL ARCHITECTURE

MEDGPT-OSS follows a modular multimodal architecture aligned with recent vision–language models such as LLaVA (Liu et al., 2023a; An et al., 2025) and Qwen-VL (Bai et al., 2023; 2025) series. Our model is composed of three core components: (1) a visual encoder for extracting image features; (2) a projection module that maps visual embeddings into the language space; and (3) a language backbone adapted from open-weight large language models.

Visual Encoder. Following established paradigms in medical MLLMs (Liu et al., 2023b; Chen et al., 2024; Xu et al., 2025; Jiang et al., 2025), we employ the CLIP-ViT-L/14@336px (Radford et al., 2021) as our primary vision backbone. This architecture was selected to strike an optimal balance between granular representational capacity and computational efficiency during inference. To bridge the modality gap, input medical images ranging from radiographs to histopathology slides are mapped into a high-dimensional latent space and subsequently aligned with the LLM’s embedding space via a projection layer.

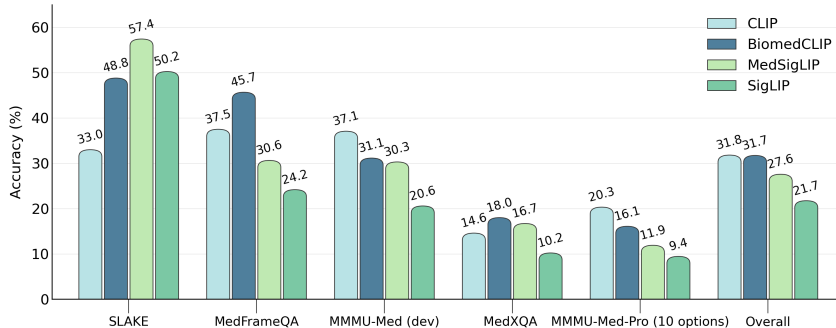


Figure 1: Preliminary evaluation of visual encoders on medical multimodal benchmarks. As an initial investigation, we compared the vanilla CLIP backbone against domain-specific alternatives (BiomedCLIP, MedSigLIP) and SigLIP. The models utilize a GPT-oss-20B trained via LoRA (2-stage training following vanilla LLaVA, where we first pretrain the projector, then fine-tune the projector and LLM backbone).

Although domain-specific encoders are tailored for clinical contexts, our selection of the vanilla CLIP backbone is substantiated by empirical benchmarking as shown in Figure 1. Specifically, we conducted a comparative ablation study utilizing a 20B-parameter model variant trained via low-rank adaptation (LoRA) (Hu et al., 2022). This evaluation leveraged the comprehensive BiomedGPT training corpus (Zhang et al., 2024), comprising 1 million multimodal pairs and 9 billion tokens of biomedical text. Our results demonstrate that vanilla CLIP consistently outperformed specialized alternatives, including BiomedCLIP (Zhang et al., 2025b), SigLIP (Zhai et al., 2023), and MedSigLIP (Sellergren et al., 2025), suggesting that the broader visual priors captured during large-scale general pretraining may provide a more resilient foundation for downstream medical reasoning.

Projection Module. Architectural choices for the projection module typically follow two primary paradigms: (1) Bottlenecked attention mechanisms, such as the Q-Former (Li et al., 2023; Carion et al., 2020), which minimize trainable parameters but may inadvertently impair spatial grounding due to the information loss inherent in fixed-length query pooling and unstable training dynamics (Yao et al., 2024); and (2) Direct projection layers (Liu et al., 2023a; Yuan et al., 2023). We opt for the latter, employing a two-layer multi-layer perceptron (MLP) that directly maps CLIP visual features into the language model’s input embedding space.

LLM Backbone. For the linguistic core of MEDGPT-OSS, we employ GPT-oss in its 20B (full parameters) configuration Agarwal et al. (2025). These models were selected for their state-of-the-art performance on clinical reasoning benchmarks, notably surpassing comparable open-weight models in factual grounding and domain-specific coherence Arora et al. (2025).

Beyond their specialized capacity for high-fidelity medical instruction-following, these variants represent an optimal trade-off within the current scaling landscape. The 20B configuration facilitates high-performance deployment on commodity hardware. By utilizing these backbones, MEDGPT-OSS retains robust general-purpose capabilities, ensuring it remains a versatile MLLM across diverse clinical scenarios. Furthermore, this open-weight architecture democratizes access to elite medical AI, empowering clinical institutions to maintain local data control and reducing reliance on high-resource cloud infrastructure.

3.2 TRAINING STRATEGIES

We implement a multi-stage or curriculum learning pipeline designed to progressively bridge the domain gap between general-purpose vision-language representations and specialized clinical requirements. All data of training phase are preventing overlap with evaluation data and avoiding potential leakage, details in Table 1.

Table 1: Overview of MEDGPT-OSS training datasets.

Modality	Dataset	No. examples	Training stages	Description
Text-only	II-Medical-Reasoning	2,197,741	IT	(R) Clinical dialogues & QA pairs
	Infinity-Instruct-Gen	1,483,097	IT	General high-quality chat instructions
	ReasonMed	1,111,555	IT	(R) Medical QA data
	MedMCQA	182,822	IT	Indian medical entrance exam questions
	HealthCareMagic-100k	112,165	IT	Real conversations between patients and doctors
	MedQA	10,178	IT	USMLE style exam questions
	MedExpQA	434	IT	Spanish medical residency exam questions
	PubMedQA	1,000	IT	Biomedical QA compiled from PubMed abstracts
	AlpaCare-MedInstruct-52k	52,002	IT	Synthetic medical instruction data curated from 167 clinical-craft tasks
	MedQuAD	47,441	IT	Medical QA pairs created from 12 NIH websites
	Huotuo-o1	40,644	IT	(R) Verifiable QA pairs from exam questions
	MedReason	32,682	IT	(R) Clinical QA with structured reasoning
	Medical-R1-Distill-Data	22,000	IT	(R) Medical reasoning distilled from Deepseek-R1
	MedThoughts-8K	7,716	IT	(R) Distilled reasoning based on MedQA data
iCliniq-10K	7,321	IT	Real patient-doctor conversation	
Radiology	ROCOv2 (filtered)	38,861	PT	Radiological images and associated medical captions
	MIMIC-CXR (single-panel)	22,747	MT	Chest X-ray images & free-form reports
	MIMIC-CXR (multi-view & longitudinal)	146,893	MT	Chest X-ray images & free-form reports
	MIMIC-CXR-VQA	363,598	IT	Chest X-ray images & VQA pairs
	SLAKE (English)	9,835	IT	2D CT/MRI/chest X-ray images & VQA pairs
	VQA-Rad	1,793	IT	Radiology image QA pairs
Histopathology	GEMeX-ThinkVG	202,383	IT	(R) Chest X-ray images & grounded VQA pairs
	Quilt-1M (filtered)	359,725	PT	Histopathology image-caption pairs
	Quilt-VQA	107,131	IT	Histopathology VQA pairs curated from videos
Mixture	PMC-OA (filtered)	477,078	PT	Image-caption pairs from PMC Open Access Subset
	BIOMEDICA (dermatology and surgery subsets)	63,775	PT	Image-caption pairs from PMC Open Access Subset
	MedTrinity (accessible)	18,525,974	MT	Medical images & enriched annotations/captions
	PubMedVision (alignment)	646,759	MT	Image-caption pairs extracted from PubMed articles
	PMC-VQA	188,229	IT	Curated VQA pairs from PMC Open Access Subset
	OpenMM-Medical	88,996	IT	Multiple-domain multi-choice VQA pairs
	GMAI-Reasoning10K	9,965	IT	(R) Medical image reasoning covering 12 imaging modalities

PT: Pretraining, MT: Mid-training, IT: Instruction-tuning. (R): Reasoning data

Pretraining. We first pretrain on short medical image–text pairs to establish robust cross-modal alignment between heterogeneous medical imaging modalities and their corresponding textual descriptions, providing a foundation for subsequent medical knowledge integration. During this initial adaptation phase, we freeze the parameters of the LLM backbone to preserve its foundational linguistic and reasoning capabilities. Conversely, we keep the visual encoder and the projection module trainable.

The pretraining corpus is constructed from PMC-OA (Lin et al., 2023), Quilt-1M (Ikezogwo et al., 2023), ROCov2 (Rückert et al., 2024), and BIOMEDICA (dermatology and surgery subsets) (Lozano et al., 2025). To ensure high-quality, clinically relevant supervision, we restrict to single-panel images and filter out common artifacts, including visible narrators, desktop environments, pathology software interfaces, and overlaid text within images. We further remove clinically irrelevant pairs and misleading numeric content with the assistance of large language models. In total, the resulting pretraining set contains approximately 939K pairs.

Mid-training. We then perform mid-training on comprehensive, long-context image–text pairs to more fully integrate medical knowledge into the MLLM, improving its ability to recognize diverse medical concepts and generalize across clinical contexts. During this stage, we relax all architectural constraints and enable full-parameter updates across the visual encoder, projection module, and LLM backbone.

For this stage, we use MIMIC-CXR (Johnson et al., 2019) training set (real-world radiology reports’ findings section), the open-sourced subset of MedTrinity (Xie et al., 2025), and the PubMedVision (Chen et al., 2024) Alignment dataset. Since MedTrinity and PubMedVision are already curated and verified, we apply no additional preprocessing to these sources. For MIMIC-CXR, we retain single-image report pairs and additionally curate longitudinal study sets following previous works (Zhang et al., 2025a;c). The mid-training corpus comprises approximately 19M samples, which is inspired by LLaVA-OneVision-1.5 (An et al., 2025) positing that scaling high-quality data at the mid-training stage can yield state-of-the-art multimodal performance.

Instruction-tuning. In line with prevailing practices for MLLMs, we include a medical instruction-tuning stage to strengthen the model’s instruction-following as well as reasoning ability across a broad range of task directives, thereby aligning its outputs more closely with user intent. Similar to mid-training, full parameters are activated.

To ensure diversity, we curate a mixed corpus that combines medical visual instruction-tuning data with pure language instruction-tuning datasets (with and without reasoning trajectories). The resulting instruction-tuning set contains approximately 7M pairs. Note that the reasoning trajectories are generally distilled from state-of-the-art LLMs through reject sampling and refinement operations. We select multiple versions based on different datasets and models to provide diverse reasoning trajectories.

3.3 IMPLEMENTATION DETAILS

The training hyperparameters are shown in Table 2. Specifically, we trained the MEDGPT-OSS-20B medical instruction model using a three-stage recipe on $8 \times$ NVIDIA B200 GPUs, employing DeepSpeed (Rasley et al., 2020) ZeRO-3 to enable efficient distributed optimization. Unless otherwise specified, we optimized the model using AdamW (Loshchilov & Hutter, 2019) ($\beta_1 = 0.9$, $\beta_2 = 0.999$, $\epsilon = 10^{-8}$) with a weight decay of 0.05. We applied a cosine learning rate decay schedule with a warmup ratio between 0.01 and 0.03, utilizing bfloat16 precision and gradient checkpointing throughout.

Training was conducted with a maximum sequence length of 32,768. We used a per-device batch size of 16, resulting in a global batch size of 128 across the 8 GPUs (with a gradient accumulation step of 1). For long-context adaptation, we integrated YaRN RoPE (Peng et al., 2024) scaling (scaling factor of 32, $\theta = 150,000$) to extend the original context length of 4,096 to 131,072 positions.

For visual inputs, we enabled dynamic image sizing supporting up to 12 dynamic patches, enforced a 336-pixel image size with a downsampling ratio of 0.5, and included thumbnails in the visual preprocessing pipeline. Stage-wise wall-clock training times on the B200 cluster were 8 hours and 27 minutes for pretraining (1 epoch), 240 hours and 24 minutes for mid-training (1 epoch), and 86 hours and 26 minutes for instruction-tuning (1 epoch).

Table 2: Default implementation hyperparameters. LR = learning rate.

Hyperparameter	Default value
Optimizer	AdamW (DeepSpeed ZeRO-3)
LR schedule	Cosine decay with warmup ratio 0.01–0.03
Max sequence length	32,768
Per-device batch size	16 (global batch size: 128)
Projector LR (stage 0)	1×10^{-3} (LLM frozen)
LLM LR (mid-training)	2×10^{-5}
LLM LR (instruction tuning)	8×10^{-5}
Vision encoder	Frozen in stage 0–1; jointly trained in stage 2
Weight decay	0.05
Precision	bfloat16 with gradient checkpointing

4 EXPERIMENTS

4.1 DATASETS

We comprehensively evaluate MEDGPT-OSS across core capability dimensions commonly reported in recent medical foundation model studies, covering multimodal reasoning, biomedical knowledge, report generation, and in-context learning. The details of each data are listed in Table 3.

Visual Question Answering (VQA). We benchmark multimodal medical reasoning on six representative datasets using their official evaluation splits unless otherwise specified: SLAKE (Liu et al., 2021), MedFrameQA (Yu et al., 2025), MMMU-Med (dev) (Yue et al., 2024), MMMU-Pro-Med (4- and 10-option test sets) (Yue et al., 2025), and MedXQA (multimodal) (Zuo et al., 2025). The

MMMU(-Pro)-Med benchmark is constructed by aggregating the clinically relevant subject subsets from MMMU(-Pro), including *basic medical science, clinical medicine, diagnostics and laboratory medicine, pharmacy, and public health*.

To ensure fair and reproducible evaluation, we standardize all tasks into closed-ended multiple-choice formats where applicable. This avoids reliance on LLM-as-a-Judge protocols, which are known to introduce bias and evaluation instability (Ye et al., 2025). All results are therefore computed via exact-match accuracy under structured answer constraints.

Table 3: Overview of MEDGPT-OSS evaluation datasets.

Task	Dataset	No. Images	No. Examples	OOD [†]
VQA	MedXQA (multimodal)	1.43 ± 1.04	2,000	✓
	SLAKE (English)	1.00 ± 0.00	836	-
	MedFrameQA	3.24 ± 1.26	2,851	✓
	MMMU-Med (dev)	1.05 ± 0.29	175	✓
	MMMU-Med-Pro (4 or 10 options)	1.14 ± 0.57	286	✓
Text QA	MedQA	-	1,273	-
	MedMCQA	-	4,183	-
	PubMed QA	-	500	-
	MMLU-Med	-	1,395	-
	MedXQA (text-only)	-	2,450	✓
	Medbullets	-	298	-
Report generation	MIMIC-CXR (multi-view & longitudinal)	4.30 ± 0.62	2,231	-
In-context learning *	Patient-trial	-	4,936	✓
	Impression generation	3.39 ± 0.64	1,564	✓

[†] OOD: Out of Distribution; * Data statistics are derived from the few-shot configurations.

Text-only Question Answering. We assess clinical and biomedical reasoning using MedQA (Jin et al., 2021), PubMedQA (Jin et al., 2019), MedMCQA (Pal et al., 2022), MedXQA (text-only), MMLU-Med (Hendrycks et al., 2021), and MedBullets (Chen et al., 2025). MMLU-Med integrates seven MMLU subsets: *anatomy, clinical knowledge, college biology, college medicine, medical genetics, nutrition, and professional medicine*. Consistent with the VQA evaluation protocol, all tasks are curated into standardized multiple-choice settings to enable objective scoring and eliminate generative evaluation ambiguity.

Report Generation. For structured medical generation, we evaluate chest X-ray findings generation on the MIMIC-CXR benchmark (including multi-view and longitudinal settings) (Zhang et al., 2025a). We report three preliminary metrics to assess clinical correctness and linguistic quality.

In-Context Learning (ICL). Beyond standard zero-shot benchmarking, we explicitly evaluate the in-context learning capability of MEDGPT-OSS, measuring its ability to leverage limited task-specific demonstrations to generalize to unseen or unfamiliar medical tasks. We report both zero-shot and few-shot performance.

For multimodal ICL, we curate a chest X-ray impression generation task based on MIMIC-CXR that is not included in the model’s training corpus, enabling evaluation of out-of-distribution task adaptation. We construct the dataset by pairing each study’s radiograph(s) with its corresponding reference *Impression* section, joining image records and textual annotations via study identifiers. Each instance is formulated as an image-conditioned generation task, optionally augmented with structured contextual metadata to guide reporting. To ensure modality–label consistency, we exclude studies with missing impressions or unavailable image files. For in-context evaluation, we further create a 1-shot variant by prepending a randomly sampled, label-valid exemplar to the query input. The demonstration–query structure is fixed under a controlled random seed to ensure reproducibility.

We further incorporate patient–trial matching benchmarks derived from the SIGIR 2016 Clinical Trials corpus (Koopman & Zuccon, 2016) and the 2021 and 2022 TREC Clinical Trials Tracks (Soboroff, 2021; Roberts et al., 2022), evaluating the model’s ability to reason over structured clinical context for eligibility determination under minimal supervision. For each patient query, we pair the patient note with retrieved candidate trials and retain only patient–trial pairs with official relevance judgments in the released qrels. Relevance grades are mapped to eligibility labels following a deterministic scheme (2/1/0 → eligible/partially eligible/not eligible). To improve interpretability

and evidence localization, patient notes are standardized via sentence segmentation with explicit sentence identifiers. Trial documents are transformed into structured prompts containing the trial title, target diseases, interventions, summary, and cleaned inclusion/exclusion criteria (with headers, bullet/number prefixes, and trivial fragments removed). Each retained patient–trial pair is formatted as a multiple-choice eligibility question. The answer set consists of four fixed options: *eligible*, *partially eligible*, *not eligible*, and *not enough information*. Option ordering is randomized per instance under a fixed deterministic seed to ensure reproducibility.

4.2 BASELINES

We compare MEDGPT-OSS-20B against most recent open-source MLLMs, with an emphasis on size-matched baselines to ensure fair comparison at the 20B+ scale. These baselines span diverse backbone families and design paradigms in medical AI.

MedGemma-27B (Sellergren et al., 2025) is trained for medical text and image comprehension using a SigLIP (Zhai et al., 2023) vision encoder pre-trained on de-identified medical datasets, and demonstrates strong baseline performance on clinically relevant benchmarks including question answering and report generation.

Lingshu-32B (Xu et al., 2025) is an open-source medical MLLM built on the Qwen2.5-VL backbone, specialized via a staged “shallow-to-deep” medical adaptation pipeline: vision–language medical alignment on curated image–text pairs, followed by medical instruction tuning (and an optional reinforcement learning variant) to strengthen clinically grounded multimodal reasoning across diverse imaging modalities.

Hulu-Med-32B is a generalist medical vision–language model that combines a SigLIP-family vision encoder with a Qwen-based language decoder, bridged by a multimodal projector and trained via a progressive multimodal curriculum to support medical understanding across 2D images, 3D volumes, videos, and clinical text (Jiang et al., 2025).

We also include additional open medical models such as **OctoMed-7B** (Ossowski et al., 2025) and **QoQ-Med-32B** (Dai et al., 2025), which represent alternative design trade-offs in training data composition and multimodal fusion strategies.

Collectively, these baselines cover a spectrum of architectural choices (e.g., Gemma-based, Qwen-based, and other backbones) and multimodal training paradigms, providing a comprehensive context for evaluating the merits and limitations of MEDGPT-OSS.

4.3 INFERENCE AND SCORING

All results reported in this paper are generated using our own inference harness with publicly released checkpoints; no numbers are copied from original publications due to the data difference. To ensure standardized and reproducible evaluation, we (i) convert each benchmark into a unified chat-style prompt format, (ii) apply the official chat template for each model when available, and (iii) implement dataset-specific post-processing and scoring rules consistent with their original definitions.

Decoding. For baseline models, we replicate the official inference guidelines and publicly released codebases, including recommended hyperparameters and decoding configurations. Unless otherwise specified, we perform a single deterministic decode per example on all medical benchmarks, matching the evaluation philosophy adopted by the original works. No sampling-based reruns or majority voting are used.

Multiple-choice scoring. For multiple-choice tasks, we employ rule-based option extraction under structured answer constraints. Prompts explicitly specify answer options, and predictions are considered correct only if they exactly match one of the valid choices. Outputs that do not correspond to any predefined option are counted as incorrect, as instruction adherence is treated as part of the model’s capability. This strict exact-match protocol avoids subjective interpretation and ensures fair, fully automated scoring.

Chest X-ray report assessment. Evaluating the quality of generated radiology reports is inherently challenging: widely used general-purpose NLP metrics (e.g., n-gram overlap or generic semantic similarity) often penalize harmless paraphrases while failing to adequately capture clinically critical errors such as missed findings or incorrect negation. As a result, the field has increasingly adopted clinically informed evaluation metrics that aim to better reflect medical correctness and utility. In this work, we use the following metrics for report quality measurement: **RadGraph-F1** (Jain et al., 2021)¹ considers literal entity agreement considering the positive or negative context of each entity. **RadCliQ** (Yu et al., 2023)² is a composite metric designed to better align with radiologists by combining multiple signals (including clinically grounded graph-based overlap) into a single quality estimate. **RaTEScore** (Zhao et al., 2024b) is inspired by the RadGraph metric but performs radiology-entity semantic matching with embedding-based similarity (e.g., cosine similarity) under an F1-like formulation, making it robust to paraphrases and synonyms while remaining sensitive to negation.

4.4 RESULTS

Medical visual question answering: Table 4 evaluates MEDGPT-OSS-20B against state-of-the-art open-weight models. Crucially, among these datasets, only SLAKE represents in-domain data; *all other benchmarks strictly evaluate out-of-distribution generalization.*

Despite its smaller 20B parameter footprint and the challenge of unseen distributions, MEDGPT-OSS-20B establishes new state-of-the-art (SOTA) results on multiple OOD benchmarks. It dominates MedFrameQA (63.01%), MMMU-dev (61.49%), and completely eclipses the 32B models on MedXQA (49.23%, a massive +14.88% absolute gain over the next best model).

On the benchmarks where it does not claim first place, MEDGPT-OSS-20B still effectively secures second place with only fractional performance reductions compared to the leading 32B model (Lingshu-32B). For instance, the gap to SOTA is a negligible -0.33% on MMMU-Med-Pro (4 opt) and -0.71% on the in-domain SLAKE. This is particularly impressive given Lingshu-32B’s explicit training advantage on the MMMU-Med development set.

Table 4: VQA results on multiple-choice benchmarks. Scores are reported in accuracy (%).

Dataset	MEDGPT-OSS	OctoMed	Hulu-Med	Lingshu [†]	MedGemma	QoQ-Med
MedXQA (multimodal)	49.23	25.60	34.35	31.43	30.90	29.64
SLAKE	71.53	65.07	69.14	72.24	55.98	46.53
MedFrameQA	63.01	42.82	62.82	61.01	47.63	55.73
MMMU-Med (dev)	61.49	47.65	57.71	59.43	47.43	51.84
MMMU-Med-Pro (4 opt)*	52.34	44.62	52.45	52.67	45.80	46.93
MMMU-Med-Pro (10 opt)	39.94	23.07	37.41	43.45	36.71	38.12

[†] Lingshu trained on the MMMU-Med dev set; * opt = options.

Medical text-only question-answering: Table 5 details the evaluation of MEDGPT-OSS-20B across standard text-only medical question-answering benchmarks. We compare our model against the same suite of open-weight and proprietary models to establish its baseline clinical knowledge and text-based reasoning capabilities.

Despite its smaller 20B parameter footprint, MEDGPT-OSS-20B achieves new state-of-the-art results on the two most reasoning-intensive benchmarks in our evaluation suite. It claims first place on Medbullets (68.71%), a dataset specifically designed to emulate challenging, real-world USMLE Step 2 & 3 clinical scenarios. More notably, it achieves SOTA on the notoriously difficult MedXQA benchmark (25.38%), successfully outperforming all 32B and 27B models on tasks requiring deep, multi-step medical logic.

¹By default, we utilize the “partial” reward level to allow for partial credit based on semantic overlap, offering a more nuanced evaluation than strict exact matching.

²The original RadCliQ metric is designed to be lower-is-better. To ensure consistency with other metrics that indicate better performance with higher values, we first calculate the average RadCliQ-v1 score for each model across the dataset and then take its reciprocal (1/RadCliQ-v1).

On foundational knowledge retrieval benchmarks, MEDGPT-OSS-20B remains highly competitive, maintaining a tight margin against significantly larger models. On MedQA (70.11%) and MMLU-Med (72.59%), it trails the leading 32B models (Hulu-Med and Lingshu) but consistently outperforms the comparably sized MedGemma-27B. This demonstrates that MEDGPT-OSS-20B successfully preserves broad medical factual recall while simultaneously optimizing for the complex clinical reasoning required to excel on datasets like MedXQA.

Table 5: Text-only medical QA results. Scores are accuracy (%).

Dataset	MEDGPT-OSS	OctoMed	Hulu-Med	Lingshu	MedGemma	QoQ-Med
MedQA	70.11	44.97	77.18	70.71	66.75	55.25
PubMedQA	57.81	48.31	61.00	62.44	55.80	42.80
MedMCQA	62.53	55.32	72.75	65.27	65.48	51.42
MedXQA (text)	25.38	10.86	23.47	21.47	14.37	8.78
MMLU-Med	72.59	61.65	87.10	82.68	80.65	74.98
Medbullets	68.71	32.21	67.45	58.69	51.34	37.25

Chest X-ray report generation: Figure 2 illustrates the performance of MEDGPT-OSS-20B on the MIMIC-CXR benchmark compared to baselines. While the larger 32B-parameter models (Hulu-Med and Lingshu) establish the upper bound for this long-form generation task, MEDGPT-OSS-20B demonstrates highly competitive performance, firmly securing the third position across all three metrics. Specifically, it achieves a RadGraph-F1 of 0.189, a RaTEScore of 0.522, and a 1/RadCliQ-v1 score of 0.803. Notably, MEDGPT-OSS maintains a narrow performance gap with the 32B models while substantially outperforming other comparably sized or open-weight alternatives. For instance, it roughly doubles the RadGraph-F1 score of MedGemma-27B (0.095) and significantly exceeds OctoMed (0.129). These results highlight that our 20B model successfully preserves high clinical fidelity and minimizes entity-level omissions during complex multimodal generation.

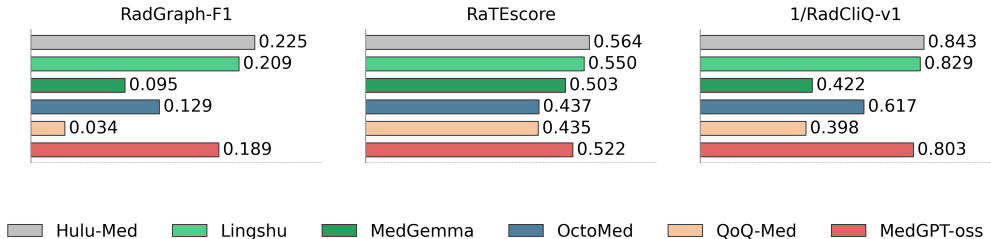


Figure 2: Evaluation of multi-view and longitudinal chest X-ray report generation on the MIMIC-CXR benchmark. Performance is measured across three clinically grounded metrics.

In-context Learning Ability. Table 6 presents a systematic evaluation of in-context learning (ICL) and clinically grounded matching capabilities across the Patient-trial and Impression benchmarks. In the zero-shot setting, MEDGPT-OSS establishes a strong baseline, achieving state-of-the-art performance on the Impression generation task (47.22%).

The distinct advantage of MEDGPT-OSS becomes evident in few-shot evaluation, where ICL inherently measures a model’s capacity to leverage provided demonstrations for solving unseen, out-of-distribution tasks. Given a single in-context example on Patient-trial, MEDGPT-OSS effectively assimilates the contextual signal, yielding a substantial performance gain from 48.81% (0-shot) to a state-of-the-art 55.60% (1-shot). Notably, the model processes these raw multimodal examples directly without any auxiliary visual guidance, underscoring the robustness of its native multimodal reasoning.

This strong context utilization stands in stark contrast to competing baselines, which frequently exhibit negative transfer upon the introduction of additional demonstrations. Specifically, Hulu-Med regresses from 51.01% to 47.00% on Patient-trial, and Lingshu similarly declines from 43.80% to 40.27% on Impression when transitioning from zero-shot to one-shot regimes; OctoMed exhibits

analogous degradation across multiple benchmarks. These results suggest that while baseline models are actively distracted by rather than benefiting from extended context, MEDGPT-OSS demonstrates a genuinely superior capacity to integrate and reason over novel contextual evidence for OOD clinical tasks.

Table 6: Few-shot benchmarks. Scores are reported as accuracy percentages (%), with the exception of the Impression benchmark, which is evaluated using RaTEScore.

Dataset	MEDGPT-OSS	OctoMed	Hulu-Med	Lingshu	MedGemma	QoQ-Med
Patient-trial (0-shot)	48.81	40.96	51.01	52.07	31.03	45.20
Patient-trial (1-shot)	55.60	40.02	47.00	48.91	52.24	47.41
Impression (0-shot)	47.22	31.04	43.14	43.80	38.42	41.44
Impression (1-shot)	47.25	30.91	41.52	40.27	38.29	40.71

5 DISCUSSION

Our current results indicate that a modular medical VLM recipe, a strong open language model (GPT-oss) coupled with a lightweight vision front-end, can achieve competitive performance across heterogeneous biomedical tasks when paired with a staged training curriculum.

Despite these promising results, several critical limitations remain. Primarily, MEDGPT-OSS is positioned as a research foundation rather than a drop-in clinical tool. Safe real-world deployment necessitates rigorous external validation to account for domain shifts across different healthcare institutions and imaging hardware. Additionally, while our model shows strong factual grounding, the generation of long-form clinical text (such as radiology reports) remains susceptible to subtle hallucinations or omissions of complex findings, a persistent challenge in medical VLMs. Finally, continuous monitoring and auditing are required to address fairness and mitigate inherent biases present in the underlying training corpora.

To address these limitations and advance the capabilities of generalist biomedical AI, we outline several key directions for future development:

Scaling Model Parameters: While our 20B configuration offers a strong balance of performance and deployability, we plan to systematically scale the underlying language backbone and visual encoders. Exploring larger dense architectures could unlock deeper clinical reasoning and broader zero-shot and few-shot generalization (Kaplan et al., 2020).

Incorporating Native 3D Image Processing: Currently, MEDGPT-OSS relies on 2D visual feature extraction. Clinical decision-making frequently depends on volumetric imaging, such as CT and MRI scans (Wasserthal et al., 2023; Zhao et al., 2024a). We aim to integrate native 3D vision encoders to process spatial depth and temporal sequences, providing a more holistic understanding of complex radiological studies.

Reinforcement Learning with Clinical Rubrics: To further align report generation with expert radiologist standards, we plan to implement reinforcement learning (e.g., RLHF or RLAI) (Ouyang et al., 2022; Bai et al., 2022). By utilizing clinically informed rubrics and metrics as reward signals, we can directly penalize critical omissions, incorrect negations, and clinical hallucinations (Zhang et al., 2025a).

Agentic Ability Training: Clinical workflows are inherently interactive. We aim to transition MEDGPT-OSS from a passive question-answering system into a domain-specific clinical agent (Zhang et al., 2026). By training the model to utilize external tools (e.g., querying electronic health records, executing medical calculators, or retrieving literature), it could support complex, multi-step clinical reasoning and longitudinal patient management (Team et al., 2026).

ACKNOWLEDGEMENTS

We gratefully acknowledge the University of Florida Research Computing for providing the HiPer-Gator supercomputing infrastructure and technical support that fundamentally enabled the research results reported in this work.

REFERENCES

- Sandhini Agarwal, Lama Ahmad, Jason Ai, Sam Altman, Andy Applebaum, Edwin Arbus, Rahul K Arora, Yu Bai, Bowen Baker, Haiming Bao, et al. gpt-oss-120b & gpt-oss-20b model card. *arXiv preprint arXiv:2508.10925*, 2025.
- Xiang An, Yin Xie, Kaicheng Yang, Wenkang Zhang, Xiuwei Zhao, Zheng Cheng, Yirui Wang, Songcen Xu, Changrui Chen, Didi Zhu, et al. Llava-onevision-1.5: Fully open framework for democratized multimodal training. *arXiv preprint arXiv:2509.23661*, 2025.
- Rahul K Arora, Jason Wei, Rebecca Soskin Hicks, Preston Bowman, Joaquin Quiñonero-Candela, Foivos Tsimpourlas, Michael Sharman, Meghan Shah, Andrea Vallone, Alex Beutel, et al. Health-bench: Evaluating large language models towards improved human health. *arXiv preprint arXiv:2505.08775*, 2025.
- Jinze Bai, Shuai Bai, Yunfei Chu, Zeyu Cui, Kai Dang, Xiaodong Deng, Yang Fan, Wenbin Ge, Yu Han, Fei Huang, et al. Qwen technical report. *arXiv preprint arXiv:2309.16609*, 2023.
- Shuai Bai, Yuxuan Cai, Ruizhe Chen, Keqin Chen, Xionghui Chen, Zesen Cheng, Lianghao Deng, Wei Ding, Chang Gao, Chunjiang Ge, Wenbin Ge, Zhifang Guo, Qidong Huang, Jie Huang, Fei Huang, Binyuan Hui, Shutong Jiang, Zhaohai Li, Mingsheng Li, Mei Li, Kaixin Li, Zicheng Lin, Junyang Lin, Xuejing Liu, Jiawei Liu, Chenglong Liu, Yang Liu, Dayiheng Liu, Shixuan Liu, Dunjie Lu, Ruilin Luo, Chenxu Lv, Rui Men, Lingchen Meng, Xuancheng Ren, Xingzhang Ren, Sibao Song, Yuchong Sun, Jun Tang, Jianhong Tu, Jianqiang Wan, Peng Wang, Pengfei Wang, Qiuyue Wang, Yuxuan Wang, Tianbao Xie, Yiheng Xu, Haiyang Xu, Jin Xu, Zhibo Yang, Mingkun Yang, Jianxin Yang, An Yang, Bowen Yu, Fei Zhang, Hang Zhang, Xi Zhang, Bo Zheng, Humen Zhong, Jingren Zhou, Fan Zhou, Jing Zhou, Yuanzhi Zhu, and Ke Zhu. Qwen3-vl technical report. *arXiv preprint arXiv:2511.21631*, 2025.
- Yuntao Bai, Saurav Kadavath, Sandipan Kundu, Amanda Askell, Jackson Kernion, Andy Jones, Anna Chen, Anna Goldie, Azalia Mirhoseini, Cameron McKinnon, et al. Constitutional ai: Harmlessness from ai feedback. *arXiv preprint arXiv:2212.08073*, 2022.
- Nicolas Carion, Francisco Massa, Gabriel Synnaeve, Nicolas Usunier, Alexander Kirillov, and Sergey Zagoruyko. End-to-end object detection with transformers. In *European conference on computer vision*, pp. 213–229. Springer, 2020.
- Hanjie Chen, Zhouxiang Fang, Yash Singla, and Mark Dredze. Benchmarking large language models on answering and explaining challenging medical questions. In *Proceedings of the 2025 Conference of the Nations of the Americas Chapter of the Association for Computational Linguistics: Human Language Technologies (Volume 1: Long Papers)*, pp. 3563–3599, 2025.
- Junying Chen, Chi Gui, Ruyi Ouyang, Anningzhe Gao, Shunian Chen, Guiming Hardy Chen, Xidong Wang, Zhenyang Cai, Ke Ji, Xiang Wan, and Benyou Wang. Towards injecting medical visual knowledge into multimodal LLMs at scale. In Yaser Al-Onaizan, Mohit Bansal, and Yun-Nung Chen (eds.), *Proceedings of the 2024 Conference on Empirical Methods in Natural Language Processing*, pp. 7346–7370, Miami, Florida, USA, November 2024. Association for Computational Linguistics. doi: 10.18653/v1/2024.emnlp-main.418. URL <https://aclanthology.org/2024.emnlp-main.418/>.
- Wei Dai, Peilin Chen, Chanakya Ekbote, and Paul Pu Liang. Qoq-med: Building multimodal clinical foundation models with domain-aware GRPO training. In *The Thirty-ninth Annual Conference on Neural Information Processing Systems*, 2025. URL <https://openreview.net/forum?id=ZwCVFBFUFb>.

- Dan Hendrycks, Collin Burns, Steven Basart, Andy Zou, Mantas Mazeika, Dawn Song, and Jacob Steinhardt. Measuring massive multitask language understanding. In *International Conference on Learning Representations*, 2021. URL <https://openreview.net/forum?id=d7KBjmI3GmQ>.
- Edward J Hu, yelong shen, Phillip Wallis, Zeyuan Allen-Zhu, Yuanzhi Li, Shean Wang, Lu Wang, and Weizhu Chen. LoRA: Low-rank adaptation of large language models. In *International Conference on Learning Representations*, 2022. URL <https://openreview.net/forum?id=nZeVKeeFYf9>.
- Wisdom Ikezogwo, Saygin Seyfioglu, Fatemeh Ghezloo, Dylan Geva, Fatwir Sheikh Mohammed, Pavan Kumar Anand, Ranjay Krishna, and Linda Shapiro. Quilt-1m: One million image-text pairs for histopathology. *Advances in neural information processing systems*, 36:37995–38017, 2023.
- Saahil Jain, Ashwin Agrawal, Adriel Saporta, Steven Truong, Du Nguyen Duong, Tan Bui, Pierre Chambon, Yuhao Zhang, Matthew P. Lungren, Andrew Y. Ng, Curtis Langlotz, and Pranav Rajpurkar. Radgraph: Extracting clinical entities and relations from radiology reports. In *Thirty-fifth Conference on Neural Information Processing Systems Datasets and Benchmarks Track (Round 1)*, 2021. URL <https://openreview.net/forum?id=pMWtc5NKd7V>.
- Songtao Jiang, Yuan Wang, Sibong Song, Tianxiang Hu, Chenyi Zhou, Bin Pu, Yan Zhang, Zhibo Yang, Yang Feng, Joey Tianyi Zhou, et al. Hulu-med: A transparent generalist model towards holistic medical vision-language understanding. *arXiv preprint arXiv:2510.08668*, 2025.
- Di Jin, Eileen Pan, Nassim Oufattole, Wei-Hung Weng, Hanyi Fang, and Peter Szolovits. What disease does this patient have? a large-scale open domain question answering dataset from medical exams. *Applied Sciences*, 11(14):6421, 2021.
- Qiao Jin, Bhuwan Dhingra, Zhengping Liu, William Cohen, and Xinghua Lu. Pubmedqa: A dataset for biomedical research question answering. In *Proceedings of the 2019 conference on empirical methods in natural language processing and the 9th international joint conference on natural language processing (EMNLP-IJCNLP)*, pp. 2567–2577, 2019.
- Alistair EW Johnson, Tom J Pollard, Seth J Berkowitz, Nathaniel R Greenbaum, Matthew P Lungren, Chih-ying Deng, Roger G Mark, and Steven Horng. Mimic-cxr, a de-identified publicly available database of chest radiographs with free-text reports. *Scientific data*, 6(1):317, 2019.
- Jared Kaplan, Sam McCandlish, Tom Henighan, Tom B Brown, Benjamin Chess, Rewon Child, Scott Gray, Alec Radford, Jeffrey Wu, and Dario Amodei. Scaling laws for neural language models. *arXiv preprint arXiv:2001.08361*, 2020.
- Bevan Koopman and Guido Zuccon. A test collection for matching patients to clinical trials. In *Proceedings of the 39th International ACM SIGIR conference on Research and Development in Information Retrieval*, pp. 669–672, 2016.
- Jason J. Lau, Soumya Gayen, Asma Ben Abacha, and Dina Demner-Fushman. A dataset of clinically generated visual questions and answers about radiology images. *Scientific Data*, 5:180251, 2018. doi: 10.1038/sdata.2018.251.
- Junnan Li, Dongxu Li, Silvio Savarese, and Steven Hoi. Blip-2: Bootstrapping language-image pre-training with frozen image encoders and large language models. In *International conference on machine learning*, pp. 19730–19742. PMLR, 2023.
- Weixiong Lin, Ziheng Zhao, Xiaoman Zhang, Chaoyi Wu, Ya Zhang, Yanfeng Wang, and Weidi Xie. Pmc-clip: Contrastive language-image pre-training using biomedical documents. In *International Conference on Medical Image Computing and Computer-Assisted Intervention*, pp. 525–536. Springer, 2023.
- Bo Liu, Li-Ming Zhan, Li Xu, Lin Ma, Yan Yang, and Xiao-Ming Wu. Slake: A semantically labeled knowledge-enhanced dataset for medical visual question answering. In *2021 IEEE 18th International Symposium on Biomedical Imaging (ISBI)*, pp. 1–5, 2021. doi: 10.1109/ISBI48211.2021.9433885.

- Haotian Liu, Chunyuan Li, Qingyang Wu, and Yong Jae Lee. Visual instruction tuning. *Advances in neural information processing systems*, 36:34892–34916, 2023a.
- Haotian Liu, Qing Liu, Amit D. Sudarshan, Mert R. Sabuncu, Marinka Zitnik, Li Fei-Fei, Jure Leskovec, and Bo Wang. Llava-med: Training a large language-and-vision assistant for biomedicine in one day, 2023b. URL <https://arxiv.org/abs/2310.03744>.
- Ilya Loshchilov and Frank Hutter. Decoupled weight decay regularization. In *International Conference on Learning Representations*, 2019. URL <https://openreview.net/forum?id=Bkg6RiCqY7>.
- Alejandro Lozano, Min Woo Sun, James Burgess, Liangyu Chen, Jeffrey J Nirschl, Jeffrey Gu, Ivan Lopez, Josiah Akililu, Anita Rau, Austin Wolfgang Katzer, et al. Biomedica: An open biomedical image-caption archive, dataset, and vision-language models derived from scientific literature. In *Proceedings of the Computer Vision and Pattern Recognition Conference*, pp. 19724–19735, 2025.
- Ming Y. Lu, Drew F. K. Williamson, Tiffany Y. Chen, Richard J. Chen, Matteo Barbieri, and Faisal Mahmood. Data-efficient and weakly supervised computational pathology on whole-slide images. *Nature Biomedical Engineering*, 2021. doi: 10.1038/s41551-020-00682-w.
- Michael Moor, Oishi Banerjee, Zahra Shakeri Hossein Abad, Harlan M Krumholz, Jure Leskovec, Eric J Topol, and Pranav Rajpurkar. Foundation models for generalist medical artificial intelligence. *Nature*, 616(7956):259–265, 2023.
- OpenAI. GPT-4 technical report. *arXiv preprint arXiv:2303.08774*, 2023.
- Timothy Ossowski, Sheng Zhang, Qianchu Liu, Guanghui Qin, Reuben Tan, Tristan Naumann, Junjie Hu, and Hoifung Poon. Octomed: Data recipes for state-of-the-art multimodal medical reasoning. *arXiv preprint arXiv:2511.23269*, 2025.
- Long Ouyang, Jeffrey Wu, Xu Jiang, Diogo Almeida, Carroll Wainwright, Pamela Mishkin, Chong Zhang, Sandhini Agarwal, Katarina Slama, Alex Ray, et al. Training language models to follow instructions with human feedback. *Advances in neural information processing systems*, 35: 27730–27744, 2022.
- Ankit Pal, Logesh Kumar Umapathi, and Malaikannan Sankarasubbu. Medmcqa: A large-scale multi-subject multi-choice dataset for medical domain question answering. In *Conference on health, inference, and learning*, pp. 248–260. PMLR, 2022.
- Bowen Peng, Jeffrey Quesnelle, Honglu Fan, and Enrico Shippole. YaRN: Efficient context window extension of large language models. In *The Twelfth International Conference on Learning Representations*, 2024. URL <https://openreview.net/forum?id=wHBfxhZulu>.
- Cheng Peng, Kai Zhang, Mengxian Lyu, Hongfang Liu, Lichao Sun, and Yonghui Wu. Scaling up biomedical vision-language models: Fine-tuning, instruction tuning, and multi-modal learning. *Journal of Biomedical Informatics*, pp. 104946, 2025.
- Alec Radford, Jong Wook Kim, Chris Hallacy, Aditya Ramesh, Gabriel Goh, Sandhini Agarwal, Girish Sastry, Amanda Askell, Pamela Mishkin, Jack Clark, et al. Learning transferable visual models from natural language supervision. In *International conference on machine learning*, pp. 8748–8763. PmLR, 2021.
- Jeff Rasley, Samyam Rajbhandari, Olatunji Ruwase, and Yuxiong He. Deepspeed: System optimizations enable training deep learning models with over 100 billion parameters. In *Proceedings of the 26th ACM SIGKDD international conference on knowledge discovery & data mining*, pp. 3505–3506, 2020.
- Kirk Roberts, Dina Demner-Fushman, Ellen M Voorhees, Steven Bedrick, and William R Hersh. Overview of the trec 2022 clinical trials track. In *TREC*, 2022.
- Alexey Romanov and Chaitanya Shivade. Lessons from natural language inference in the clinical domain. In *Proceedings of the 2018 Conference on Empirical Methods in Natural Language Processing (EMNLP)*, pp. 1586–1596, 2018. doi: 10.18653/v1/D18-1187.

- Johannes Rückert, Louise Bloch, Raphael Brüngel, Ahmad Idrissi-Yaghir, Henning Schäfer, Cynthia S Schmidt, Sven Koitka, Obioma Pelka, Asma Ben Abacha, Alba G. Seco de Herrera, et al. Rocov2: Radiology objects in context version 2, an updated multimodal image dataset. *Scientific Data*, 11(1):688, 2024.
- Andrew Sellergren, Sahar Kazemzadeh, Tiam Jaroensri, Atilla Kiraly, Madeleine Traverse, Timo Kohlberger, Shawn Xu, Fayaz Jamil, Cían Hughes, Charles Lau, et al. Medgemma technical report. *arXiv preprint arXiv:2507.05201*, 2025.
- Ian Soboroff. Overview of trec 2021. In *TREC*, 2021.
- Kimi Team, Tongtong Bai, Yifan Bai, Yiping Bao, SH Cai, Yuan Cao, Y Charles, HS Che, Cheng Chen, Guanduo Chen, et al. Kimi k2. 5: Visual agentic intelligence. *arXiv preprint arXiv:2602.02276*, 2026.
- Arun James Thirunavukarasu, Darren Shu Jeng Ting, Kabilan Elangovan, Laura Gutierrez, Ting Fang Tan, and Daniel Shu Wei Ting. Large language models in medicine. *Nature medicine*, 29(8):1930–1940, 2023.
- Tao Tu, Shekoofeh Azizi, Danny Driess, Mike Schaeckermann, Mohamed Amin, Pi-Chuan Chang, Andrew Carroll, Chuck Lau, Ryutaro Tanno, Ira Ktena, Basil Mustafa, Aakanksha Chowdhery, Yun Liu, Simon Kornblith, David Fleet, Philip Mansfield, Sushant Prakash, Renee Wong, Sunny Virmani, Christopher Semturs, S. Sara Mahdavi, Bradley Green, Ewa Dominowska, Blaise Aguera y Arcas, Joelle Barral, Dale Webster, Gregory S. Corrado, Yossi Matias, Karan Singhal, Pete Florence, Alan Karthikesalingam, and Vivek Natarajan. Towards generalist biomedical AI. *arXiv preprint arXiv:2307.14334*, 2023.
- Jakob Wasserthal, Hanns-Christian Breit, Manfred T Meyer, Maurice Pradella, Daniel Hinck, Alexander W Sauter, Tobias Heye, Daniel T Boll, Joshy Cyriac, Shan Yang, et al. Totalsegmentator: robust segmentation of 104 anatomic structures in ct images. *Radiology: Artificial Intelligence*, 5(5):e230024, 2023.
- Yunfei Xie, Ce Zhou, Lang Gao, Juncheng Wu, Xianhang Li, Hong-Yu Zhou, Sheng Liu, Lei Xing, James Zou, Cihang Xie, and Yuyin Zhou. Medtrinity-25m: A large-scale multimodal dataset with multigranular annotations for medicine. In *The Thirteenth International Conference on Learning Representations*, 2025. URL <https://openreview.net/forum?id=IwgmgidYPS>.
- Weiwen Xu, Hou Pong Chan, Long Li, Mahani Aljunied, Ruifeng Yuan, Jianyu Wang, Chenghao Xiao, Guizhen Chen, Chaoqun Liu, Zhaodonghui Li, et al. Lingshu: A generalist foundation model for unified multimodal medical understanding and reasoning. *arXiv preprint arXiv:2506.07044*, 2025.
- Xi Yang, Aokun Chen, Nima PourNejatian, Hoo Chang Shin, Kaleb E Smith, Christopher Parisien, Colin Compas, Cheryl Martin, Anthony B Costa, Mona G Flores, et al. A large language model for electronic health records. *NPJ digital medicine*, 5(1):194, 2022.
- Linli Yao, Lei Li, Shuhuai Ren, Lean Wang, Yuanxin Liu, Xu Sun, and Lu Hou. Deco: Decoupling token compression from semantic abstraction in multimodal large language models. *arXiv preprint arXiv:2405.20985*, 2024.
- Jiayi Ye, Yanbo Wang, Yue Huang, Dongping Chen, Qihui Zhang, Nuno Moniz, Tian Gao, Werner Geyer, Chao Huang, Pin-Yu Chen, Nitesh V Chawla, and Xiangliang Zhang. Justice or prejudice? quantifying biases in LLM-as-a-judge. In *The Thirteenth International Conference on Learning Representations*, 2025. URL <https://openreview.net/forum?id=3GTtZFiajM>.
- Feiyang Yu, Mark Endo, Rayan Krishnan, Ian Pan, Andy Tsai, Eduardo Pontes Reis, Eduardo Kaiser Ururahy Nunes Fonseca, Henrique Min Ho Lee, Zahra Shakeri Hossein Abad, Andrew Y Ng, et al. Evaluating progress in automatic chest x-ray radiology report generation. *Patterns*, 4(9), 2023.
- Suhao Yu, Haojin Wang, Juncheng Wu, Luyang Luo, Jingshen Wang, Cihang Xie, Pranav Rajpurkar, Carl Yang, Yang Yang, Kang Wang, et al. Medframeqa: A multi-image medical vqa benchmark for clinical reasoning. *arXiv preprint arXiv:2505.16964*, 2025.

- Zhengqing Yuan, Zhaoxu Li, Weiran Huang, Yanfang Ye, and Lichao Sun. Tinygpt-v: Efficient multimodal large language model via small backbones. *arXiv preprint arXiv:2312.16862*, 2023.
- Xiang Yue, Yuansheng Ni, Kai Zhang, Tianyu Zheng, Ruoqi Liu, Ge Zhang, Samuel Stevens, Dongfu Jiang, Weiming Ren, Yuxuan Sun, et al. Mmmu: A massive multi-discipline multimodal understanding and reasoning benchmark for expert agi. In *Proceedings of the IEEE/CVF conference on computer vision and pattern recognition*, pp. 9556–9567, 2024.
- Xiang Yue, Tianyu Zheng, Yuansheng Ni, Yubo Wang, Kai Zhang, Shengbang Tong, Yuxuan Sun, Botao Yu, Ge Zhang, Huan Sun, et al. Mmmu-pro: A more robust multi-discipline multimodal understanding benchmark. In *Proceedings of the 63rd Annual Meeting of the Association for Computational Linguistics (Volume 1: Long Papers)*, pp. 15134–15186, 2025.
- Xiaohua Zhai, Basil Mustafa, Alexander Kolesnikov, and Lucas Beyer. Sigmoid loss for language image pre-training. In *Proceedings of the IEEE/CVF international conference on computer vision*, pp. 11975–11986, 2023.
- Kai Zhang, Rong Zhou, Eashan Adhikarla, Zhiling Yan, Yixin Liu, Jun Yu, Zhengliang Liu, Xun Chen, Brian D Davison, Hui Ren, et al. A generalist vision–language foundation model for diverse biomedical tasks. *Nature Medicine*, 30(11):3129–3141, 2024.
- Kai Zhang, Christopher Malon, Lichao Sun, and Martin Renqiang Min. Editgrpo: Reinforcement learning with post-rollout edits for clinically accurate chest x-ray report generation. In *Proceedings of the 14th International Joint Conference on Natural Language Processing and the 4th Conference of the Asia-Pacific Chapter of the Association for Computational Linguistics*, pp. 304–316, 2025a.
- Kai Zhang, Corey D Barrett, Jangwon Kim, Lichao Sun, Tara Taghavi, and Krishnaram Kenthapadi. Radagents: Multimodal agentic reasoning for chest x-ray interpretation with radiologist-like workflows. In *Medical Imaging with Deep Learning*, 2026. URL <https://openreview.net/forum?id=2mlxx8R0Ru>.
- Sheng Zhang, Yanbo Xu, Naoto Usuyama, Hanwen Xu, Jaspreet Bagga, Robert Tinn, Sam Preston, Rajesh Rao, Mu Wei, Naveen Valluri, et al. A multimodal biomedical foundation model trained from fifteen million image–text pairs. *Nejm Ai*, 2(1):AIoa2400640, 2025b.
- Xi Zhang, Zaiqiao Meng, Jake Lever, and Edmond SL Ho. Libra: Leveraging temporal images for biomedical radiology analysis. In *Findings of the Association for Computational Linguistics: ACL 2025*, pp. 17275–17303, 2025c.
- Songlin Zhao, Rong Zhou, Yu Zhang, Yong Chen, and Lifang He. Normative modeling with focal loss and adversarial autoencoders for alzheimer’s disease diagnosis and biomarker identification. In *International workshop on applications of medical AI*, pp. 231–240. Springer, 2024a.
- Weike Zhao, Chaoyi Wu, Xiaoman Zhang, Ya Zhang, Yanfeng Wang, and Weidi Xie. Ratescore: A metric for radiology report generation. In *Proceedings of the 2024 Conference on Empirical Methods in Natural Language Processing*, pp. 15004–15019, 2024b.
- Yuxin Zuo, Shang Qu, Yifei Li, Zhang-Ren Chen, Xuekai Zhu, Ermo Hua, Kaiyan Zhang, Ning Ding, and Bowen Zhou. Medxpertqa: Benchmarking expert-level medical reasoning and understanding. In *International Conference on Machine Learning*, pp. 80961–80990. PMLR, 2025.